JOURNAL OF CATALYSIS 97, 177–187 (1986)

Iron Alloy Fischer–Tropsch Catalysts

V. FeCo on Y Zeolite

T-A. LIN, L. H. SCHWARTZ,[1] AND J. B. BUTT[2]

Ipatieff Laboratory and Department of Chemical Engineering, Northwestern University, Evanston, Illinois 60201

Received May 3, 1985; revised August 12, 1985

A series of Fe, Co, and FeCo catalysts on Y-zeolite support, prepared both by ion exchange and impregnation, has been investigated and compared with a previously reported (7,9) series supported on wide-pore SiO_2. Characterization methods were X-ray diffraction, H_2 and CO chemisorption, Mössbauer spectroscopy, and atomic absorption. The oxidation, reduction, and carburization behavior of the iron-containing catalysts were observed by Mössbauer spectroscopy. The reversibility of FeY (ion exchanged) in oxidation–reduction cycles was confirmed. The ion-exchanged catalysts (FeY, FeCoY) do not show any iron metal, or alloy or carbide phase after reduction or attempted carburization. In contrast with prior results with silica-supported Fe and FeCo, where there appear to be significant differences, Fe/HY (impregnated) and FeCo/HY appear quite similar in characterization by Mössbauer spectroscopy and in reaction behavior. A 1/1 : CO/H_2 feed was used to investigate the Fischer–Tropsch reaction at 1 atm and 523 K. Some additional runs were made at a total pressure of 13.6 atm. As in prior studies (Amelse, J. A., Schwartz, L. H., and Butt, J. B., *J. Catal.* **72,** 95, 1981; Arcuri, K. B., Piotrowski, R. B., Schwartz, L. H., and Butt, J. B., *J. Catal.* **85,** 349, 1984) it was found that the CO turnover frequency (N_{CO}) in general decreases with increasing CO conversion. A higher selectivity for higher molecular weight products is found for HY supported catalysts, and in all cases an approximate behavior in accord with the Schultz–Anderson distribution was observed.

INTRODUCTION

There is considerable interest in the use of zeolites as supports and/or active components in Fischer–Tropsch and related synthesis reactions (*1–3*). Bifunctional reactions and shape-selectivity effects (*4*), not anticipated with conventional supports, can be important for metal/zeolite materials.

Not much, however, has been reported for bimetallic formulations on zeolites. In this work a Faujasite-type (*5, 6*) has been used as a support for Fe, Co, and FeCo in the synthesis reaction. The results are compared with prior information obtained for similar silica-supported materials. A combination of characterization and reaction experiments was used to investigate the properties of the catalysts after various oxidation–reduction–carburization cycles. Details of the procedures involved have been reported by Amelse *et al.* (*7*).

EXPERIMENTAL

Preparation of the catalysts. The beginning support material was 80–120 mesh NaY supplied by Strem Chemicals, Inc. The surface area was 300 m^2/g and the Si/Al ratio 2.4. Two series of catalysts, prepared either by ion exchange or by impregnation, were employed in this investigation.

For the ion-exchanged materials, protonated Y (*8*), FeY, and FeCoY were obtained by exchange of the parent NaY with 0.1 *N* NH_4Cl, $FeCl_2$, and $CoCl_2$ solutions. Attainment of the final level of loading required several exchange cycles. FeY and FeCoY were exchanged at 70°C in a N_2 atmosphere to prevent Fe^{2+} oxidation to Fe^{3+} and possible substitution for Al^{3+} in the ze-

[1] Department of Materials Science and Engineering. Present address: National Bureau of Standards, Gaithersburg, Md. 20899.

[2] To whom correspondence should be addressed.

0021-9517/86 $3.00

olite lattice. These samples were then washed in deionized water until complete evolution of chloride, measured by negligible precipitation of $AgNO_3$, was attained. The final catalysts were obtained by drying in flowing N_2 at 100°C overnight. The dried NH_4Y was then further calcined at 500°C for 12 h to form HY. Atomic absorption was used to measure the final weight loading of metals on these ion-exchanged catalysts.

Impregnated catalysts, designated Fe/HY, Co/HY, and FeCo/HY were prepared using the incipient wetness technique. Before impregnation the support was calcined at 500°C overnight, then impregnated with aqueous $Fe(NO_3)_3$ or $Co(NO_3)_3$ solutions to reach the desired metal loading; these materials were again dried in air at 100°C overnight. A summary of the catalysts prepared by the two methods is given in Table 1.

Characterization of the Catalysts

X-Ray diffraction. A conventional diffractometer was employed with Ni-filtered Cu$K\alpha$ radiation at 40 kV, 30 mA. Automated point counting was employed using a step-scanning increment of 0.2° (2θ). Fourier line profile analysis was employed for estimation of metal particle size and size distribution. Although there is significant background due to the crystallinity of the zeolite, the metal loadings were sufficient to yield adequate resolution.

Mössbauer spectroscopy. Spectra were obtained with a constant acceleration Austin spectrometer coupled to a Nuclear Data-2200 multichannel analyzer. Details are given elsewhere (*7*).

Hydrogen/carbon monoxide chemisorption. Hydrogen chemisorption on the impregnated catalysts was measured using the adsorption/desorption method (*7*). The catalyst was reduced, H_2,425°,24 (this code represents hydrogen at 425°C for 24 h), then cooled H_2 to 0°C. Subsequently, the sample was allowed to equilibrate in flowing Ar and H_2 uptake measured by desorption upon reheating to 425°C. Hydrogen uptakes were not measurable on the ion-exchanged catalysts, however, detectable CO chemisorption, indicative of a small amount of iron metal, was obtained for these catalysts at 25°C using the volumetric method.

TABLE 1

Catalysts Investigated

(A) Impregnation	Fe/HY, Fe/NaY	Fe 4.94 wt%
	Co/HY, Co/NaY	Co 4.61 wt%
	FeCo/HY	Fe 3.85 wt% + Co 1.02 wt%
(B) Ion exchange	FeY	Fe 3.0 wt%
	FeCoY	Fe + Co 3.1 wt%, exchanged from 3/1 Fe/Co solution

Reaction Measurements

Turnover frequency and selectivity measurements were conducted in a conventional flow reactor at small conversions and under conditions that diffusional intrusions were not significant. Procedures are detailed in Refs. (*7, 9*). Most reaction experiments were carried out at 250 ± 1°C, 1 atm, with 1 : 1/(H_2/CO) feed, although some runs were also conducted at 13.6 atm. Total CO conversion was kept below 10 mol%. Pretreatment of catalysts was always H_2, 425°,24. Conditions of carburization for characterization were the same as for the synthesis reaction.

Characterization Results

Mössbauer spectroscopy. Mössbauer spectra were employed to determine changes in chemical states, for phase identification, and the location of the cation within the zeolite. Amelse *et al.* (*10, 11*) have reported Mössbauer spectra for a similar series of SiO_2-supported iron catalysts. Comparisons with these are given below.

FeY: reversibility of oxidation–reduction. Catalysts were treated at H_2,425°,24 with subsequent O_2,500°,24. This results in transformation from Fe^{2+} to Fe^{3+}, with further H_2,425°,24 regenerating Fe^{2+}. These results agree with those of Delgass *et al.* (*12, 13*) and Segawa *et al.* (*14*). For quantitative comparison, Mössbauer parameters are given in Table 2.

TABLE 2

Mössbauer Parameters for Reduction–Oxidation of FeY

Treatment	Phase	IS (mm/s)	QS (mm/s)
H_2,425°,24	Fe^{2+}	0.72[a]	0.63[a]
		1.12[b]	2.34[b]
O_2,500°,24	Fe^{3+}	0.71	1.08
H_2,425°,24	Fe^{2+}	0.69[a]	0.62[a]
		1.09[b]	2.29[b]

Note. IS, isomer shift; QS, quadrupole splitting.
[a] Inner peak of Fe^{2+}.
[b] Outer peak of Fe^{2+}.

Fe/HY: reduction and carburization. Fe/HY and Fe/NaY are similar in behavior and also similar to Fe/SiO_2. Characteristic Mössbauer parameters following various treatments are given in Table 3. The calcined sample gives a six-line pattern, identified as α-Fe_2O_3 (verified by X-ray diffraction), with a central doublet believed to be due to superparamagnetic oxide. The average particle size estimated from the ratio of the six-line pattern to the superparamagnetic peak (*10*) is estimated to be 13 nm. The reduced sample gives a six-line pattern and two sets of doublets, the former associated with Fe^0 while one of the doublets is the outer peak of Fe^{2+} and the other unreduced superparamagnetic oxide. After carburization 1 : 1/(H_2/CO),250°,3 the ε'-carbide phase is the only carbide observed. Fe^{2+} disappears, but oxide remains. Further details are given by Lin (*15*).

FeY: reduction and carburization. The iron catalyst prepared by ion exchange is substantially different from that prepared by impregnation. The Fe^{2+}–Fe^{3+} interconversion of the latter material is documented in Table 2. However, as shown in Fig. 1A, there is no six-line pattern observed after O_2, 500°, 24; the pattern after H_2,425°,24 is identical to that of FeY after initial reduction, and the pattern obtained after carburization, (Fig. 1B), suggests the absence of carbide phases even after 10 h of reaction (Fe/HY is converted after 3 h). Hence, after reduction or attempted carburization, Fe^{2+} is the only chemical state indicated. The outer peaks are characteristic of ferrous ions occupying the octahedral sites in the hexagonal prisms of the zeolite, while the inner peaks can be assigned to ferrous ions in the sodalite cages (*16*).

FeCo/HY: reduction and carburization. Comparison of the spectrum of calcined FeCo/HY (Fig. 2A, Table 4) with that corresponding for Fe/HY (Table 3) indicates that only a weak six-line pattern of α-Fe_2O_3 is observed. The low ratio of the six-line pattern to the superparamagnetic peak indicates a small oxide particle size for the bimetallic material. The spectrum of the reduced catalyst (Fig. 2B), is predominately that of iron metal. Previous work for Fe/SiO_2 (*9*), and separate work on Fe/H-mordenite (Si/Al ~ 10) with similar metal loading, has shown the formation of an inhomogeneous alloy under these conditions. Furthermore, those materials did not form carbide phases under synthesis conditions, while the spectrum for FeCo/HY of

TABLE 3

Room-Temperature Mössbauer Parameters for Fe/HY

Treatment	Phase	IS (mm/s)	QS (mm/s)	H^a (kOe)	Area fraction
O_2,500°,24	(1) α-Fe_2O_3	0.38	0.38	511.5	0.35
	(2) Superparamagnetic oxide	0.06	1.03	—	0.65
H_2,425°,24;	(1) ε'-Carbide	0.04	0.01	174.7	0.27
1 : 1/(H_2/CO),250°,3	(2) Superparamagnetic oxide	0.10	1.08	—	0.73

[a] Hyperfine field.

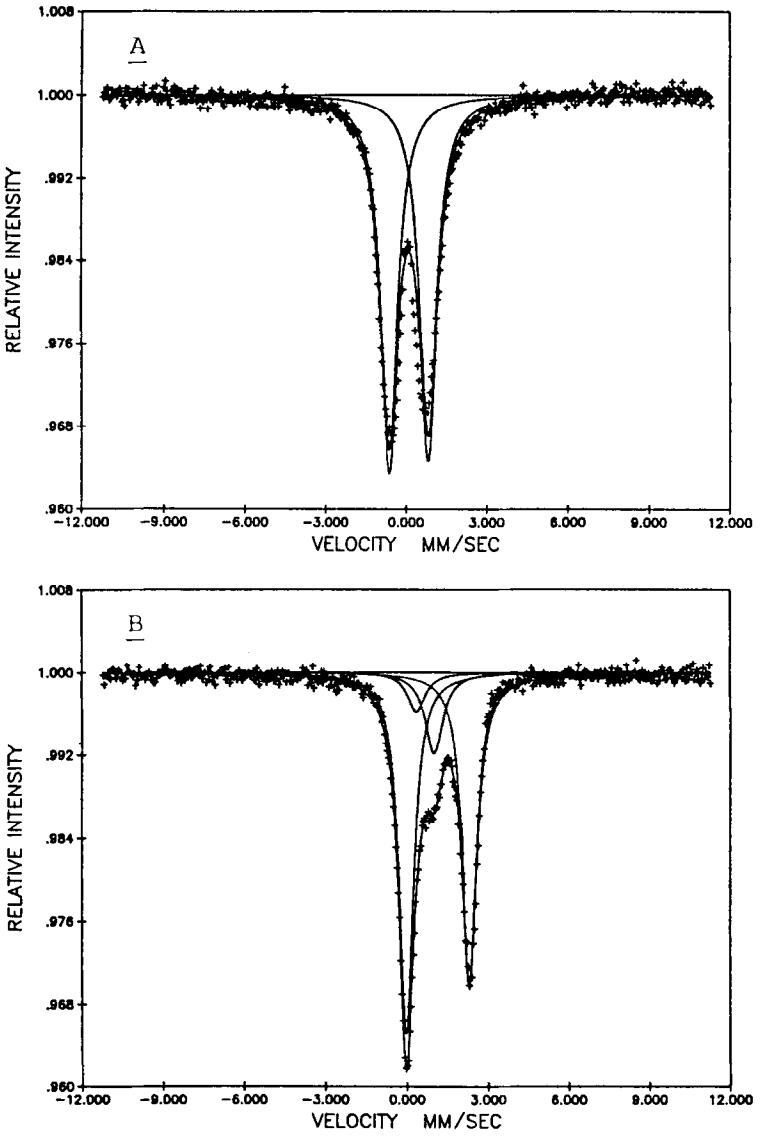

FIG. 1. The room-temperature Mössbauer spectra of FeY after (A) O_2,500°,24; (B) H_2,425°,24; 1 : 1/(H_2/CO),250°,10.

Fig. 2C indicates the formation of two carbide phases, a θ-phase (*7*) in addition to the ε'-phase. In preparation, nucleation must be such that Fe and Co ions agglomerate to form separate Fe and Co clusters, effectively suppressing alloy formation. Similar absence of alloy formation on zeolite-supported FeCo has recently been reported by Suib *et al.* (*3*).

FeCoY: reduction and carburization. Spectra for the three different treatments are shown in Fig. 3. They are quite similar to the corresponding treatments of FeY reported in Table 2. Again Fe^{2+} is the only chemical state that can be observed after reduction and carburization. There is *no* evidence of iron metal, FeCo alloy, or carbide phases in these spectra.

Catalyst particle size and percentage exposed. As stated, hydrogen uptake was

TABLE 4

Room-Temperature Mössbauer Parameters for FeCo/HY

Treatment	Phase	IS (mm/s)	QS (mm/s)	H (kOe)	Area fraction
O_2,500°,24	(1) Oxide	0.46	0.58	510.8	0.12
	(2) Superparamagnetic oxide	0.36	1.01	—	0.88
H_2,425°,24	(1) Fe^{2+}	0.96	2.43	—	0.11
	(2) Superparamagnetic oxide	0.17	0.90	—	0.30
	(3) Fe metal	0.06	0.06	333.5	0.59
1 : 1/(H_2/CO),250°,36	(1) Superparamagnetic oxide	0.21	1.03	—	0.42
	(2) ε'-Carbide	0.25	0.30	172.4	0.32
	(3) θ-Carbide	0.28	0.19	209.1	0.26

measured via a flow adsorption/desorption method for the samples prepared by impregnation. Small amounts of CO uptake were measured volumetrically for ion-exchanged samples, indicative of some possible Fe°, but the numbers have little quantitative meaning and are not reported here. In Table 5a are given the percentage exposed values based on the assumption of (1 : 1)/(H : metal) stoichiometry (*7*) and in Table 5 are results from the X-ray diffraction analysis (*17, 18*). Particle sizes were determined from the data in directions indicated and the strain broadening effect checked by observing two orders of a peak (typically 110, 220). The chemisorption particle sizes were determined from percentage exposed by calculation assuming spherical particles. There is a fair agreement between chemisorption and X-ray measurements for the impregnated catalysts. The origin of discrepancies between the two measurements is discussed in (*7*).

TABLE 5

Percentage Exposed and Particle Size

	(a) Percentage exposed by H_2 chemisorption			
Fe/HY	7.2			
Co/HY	12.5			
FeCo/HY	6.2			
	(b) Particle size, nm			
	X-Ray diffraction			Chemisorption
	⟨110⟩	⟨211⟩	Average	
Fe/HY	7.5	7.7	7.6	14.9
FeCo/HY	8.1	8.1	8.1	15.8

Activity and Selectivity

CO Activity. The CO turnover frequency, N_{CO}, is given as the molecules of CO converted to products exclusive of CO_2 per surface atom per second. This makes no claim that individual surface Fe atoms are active sites for CO turnover, only that normalization to this value is a convenient basis for relative comparisons. Table 6 presents the steady-state CO activities at 1 atm, 250°C for 1 : 1/(H_2/CO) feed after pretreatment H_2,425°,24. In general the N_{CO} values decrease with increasing conversion, as for SiO_2-supported catalysts (*9*). The Fe/HY materials are the most active, and in general the Y-supported catalysts

TABLE 6

CO Turnover Frequencies, $N_{CO\times10^{-3}}$, s^{-1}

CO Conversion	1%	2%	3%
Fe/HY	34.3	24.4	15.7
Fe/NaY	12.3	9.3	6.3
Co/HY	2.5	2.0	1.8
Co/NaY	1.1	1.0	0.9
FeCo/HY	14.2	12.3	8.1
FeY	0.7	0.6	0.6
FeCoY	0.5	0.5	0.5
Fe/SiO_2[a]	—	3.2	—
Co/SiO_2[a]	—	17.0	—
$FeCo/SiO_2$[a]	—	2.2	—

Note. All reaction data, Tables 6–8, are for 250°C, 1 : 1/(H_2/CO).

[a] Data of Arcuri *et al.* (*9*).

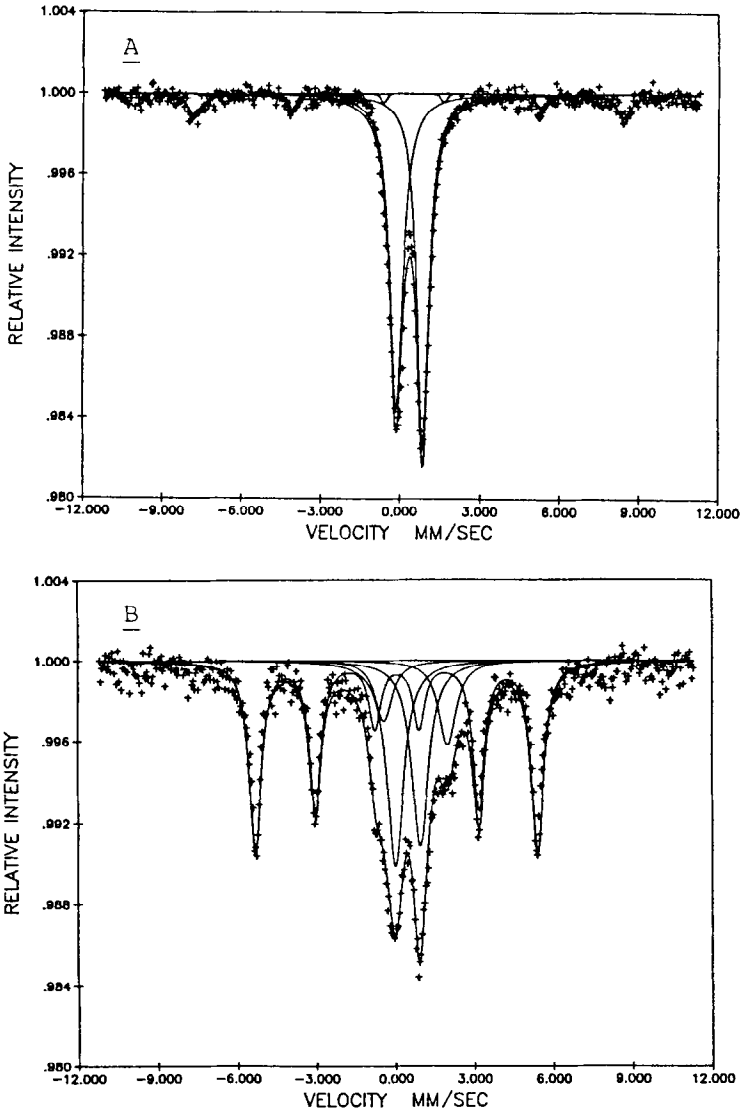

FIG. 2. The room-temperature Mössbauer spectra of FeCO/HY after (A) O_2,500°,24; (B) H_2,425°,24; (C) 1 : 1/(H_2/CO),250°,10.

prepared by impregnation are more active than the SiO_2 samples (Co/SiO_2 is an exception). Ion-exchanged preparations are of uniformly low activity.

Water–gas shift activity. The ratio of the production rates (N_{CO_2}/N_{H_2O}), is used to provide a measure of the shift activity (*7*). The Co catalysts have lower activity by this measure than either the Fe or FeCO catalysts, with the latter two having about the same activity. This agrees with results for SiO_2 catalysts (*9*), where Co is generally of lower activity. Shift activity decreases with increasing pressure, in accord with prior observation, and increases modestly with conversion. Details are provided by Lin (*15*).

Product selectivity. The product selectivities at 3 mol% conversion of CO are given in Table 7. There is a significant variation in hydrocarbon selectivity among these catalysts, with a norm of about 25% of total

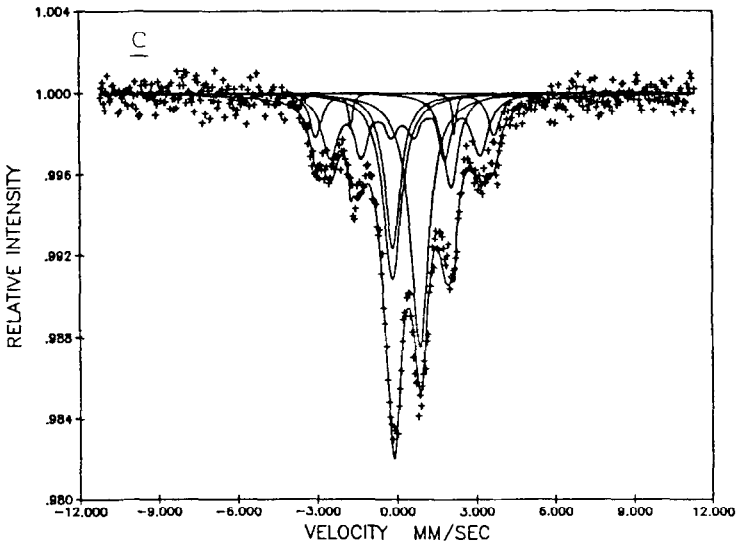

FIG. 2—*Continued.*

product showing up as hydrocarbons at 1 atm, increasing to about 35% with oxygenates (with the exception of FeCo/HY) at 13.6 atm. Substantial methanol is produced at the higher pressure (about the same in all cases), but there is no selectivity for oxygenate production at low pressures. This corresponds to that observed for SiO_2-supported materials (*9*).

Olefin/paraffin product ratios are shown as a function of conversion in Fig. 4. These decrease with conversion, as for Fe/SiO_2 and $FeCo/SiO_2$, but do not appear to be very pressure dependent where one can compare results at 1 and 13.6 atm. Catalysts prepared by impregnation on NaY, and the ion-exchanged materials, have approximately twice the olefin selectivity of those prepared by impregnation on HY. For the Na supports, this may be the result

TABLE 7

Product Composition at 3% CO Conversion

Product composition	Fe/HY	FeNaY	FeY	Co/HY	Co/NaY	FeCo/HY	FeCoY	Fe/SiO_2[b]	Co/SiO_2[b]	$FeCo/SiO_2$
CO_2	22.2,2.3	25.1	16.2	6.4,2.5[a]	6.3	25.4,22.5[a]	18.9	—	—	—
H_2O	53.0,61.8	51.8	55.4	64.4,61.3	62.4	50.2,49.8	54.8	—	—	—
CH_n = oxygenates	24.9,35.2	23.2	28.4	29.4,36.2	31.4	24.4,27.8	26.3	—	—	—
CH_n + oxygenates										
C_1	51.3,37.3	47.5	52.6	57.1,38.2	61.7	51.4,36.9	53.1	50.4	60.7	52.2
$C_2^=$	3.9,2.2	6.2	7.2	3.6,2.4	4.8	6.4,2.4	7.2	11.3	7.4	11.4
C_2	9.5,5.6	6.9	8.6	7.7,7.8	5.4	11.3,6.9	8.4	6.6	3.2	6.1
$C_3^=$	9.2,3.4	13.1	8.8	8.3,3.4	7.3	5.3,4.5	8.3	3.2	11.5	11.0
C_3	4.3,4.2	5.7	6.5	2.4,4.8	1.9	4.4,3.7	6.5	2.4	1.2	2.4
$C_4^=$	3.4,4.1	3.1	5.4	6.2,3.9	3.7	3.5,3.5	5.7	7.4	8.6	7.8
C_4	5.0,3.2	4.0	4.3	3.4,2.9	4.1	2.9,2.7	4.0			
C_5^+	14.4,14.0	10.4	6.8	11.4,13.4	8.5	14.9,13.6	6.9	7.6	7.4	7.0
MeOH	—,25.0	—	—	—,22.8	—	—,27.7	—	1.1	—	2.1
$C_2^=/C_2$	0.41,0.39	0.9	0.84	0.47,0.3	0.89	0.56,0.35	0.86	1.71	2.31	1.87

[a] Second entry for total pressure of 13.6 atm.
[b] Data of Arcuri *et al.* (*9*).

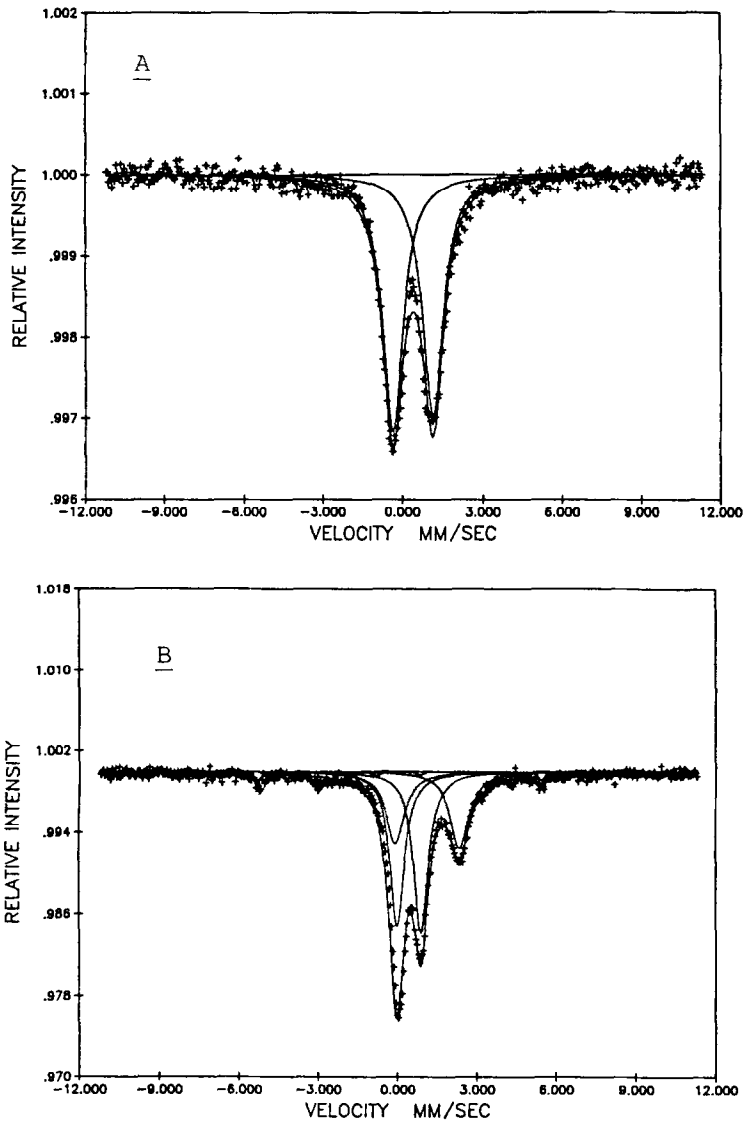

FIG. 3. The room-temperature Mössbauer spectra of FeCoY after (A) O_2,500°,24; (B) H_2,425°,24; (C) 1 : 1/(H_2/CO),250°,10.

of inhibition of formation of carbenium-like surface species and a corresponding retardation of the chain growth process. This is also reflected in the lower C_5^+ yields for NaY shown in Table 8. A major departure from prior results with SiO_2 catalysts is the appreciable yield of methanol for Co/HY at 13.6 atm. Arcuri *et al.* (*9*) reported Co/SiO_2 to be inactive for methanol formation even at elevated pressures; in the present experiment with Co/HY the methanol yield increases to almost 20% of the total product at 13.6 atm.

Chain growth. For chain growth reactions with a constant ratio of propagation to termination rates the relation between Y_j, the yield of product j, and the carbon number of the product, n, is expressed in terms of a constant α that represents the probability of chain propagation (*19*). Higher α val-

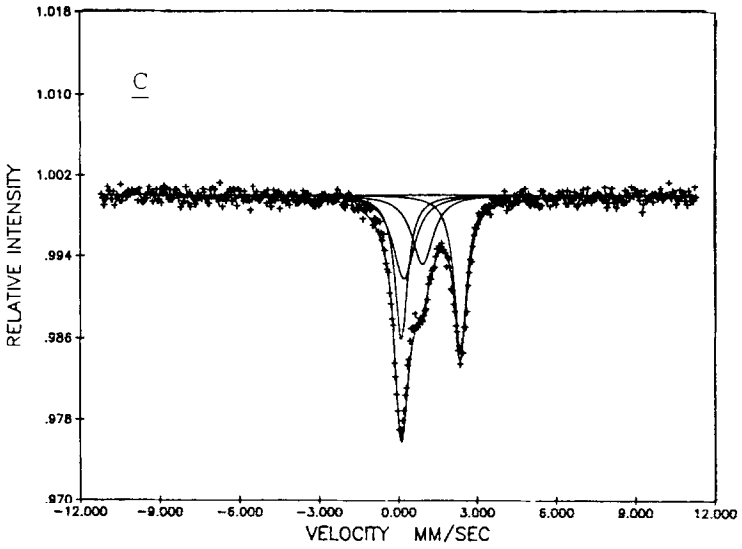

FIG. 3—*Continued.*

ues imply favored high-molecular-weight products, so comparison of α affords a convenient means for evaluation of hydrocarbon product selectivity, Based on the data reported in Table 8, the average α values give the following sequence for similar supports:

$$\text{Fe} > \text{Co} > \text{FeCo} \quad (\text{Y support})$$

$$\text{Co} > \text{FeCo} > \text{Fe} \quad (SiO_2 \text{ support})$$

If support effects are considered for an individual metallic component, then:

$$\text{HY(impregnated)} > \text{NaY(impregnated)} > SiO_2 > \text{Y(ion exchanged)}.$$

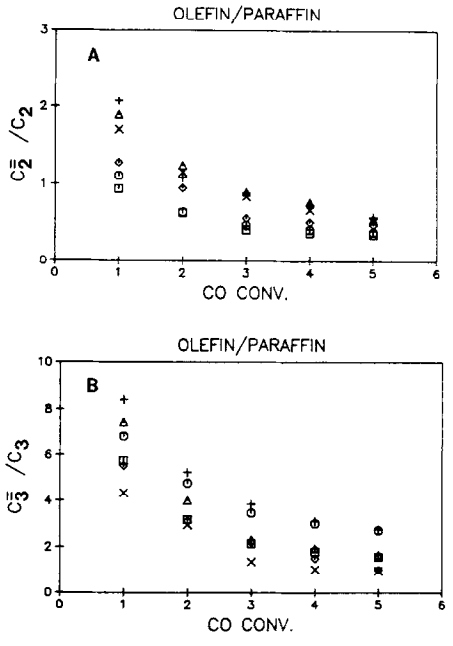

FIG. 4. Olefin/paraffin ratios as a function of CO conversion. (A) Ethylene to ethane; (B) propylene to propane. Reaction at 1 : 1/(H_2/CO),250°, 1 atm. □, Fe/HY; ○, Co/HY; △, Fe/NaY; +, Co/NaY; ×, FeY; ◇, FeCo/HY.

TABLE 8

Chain Growth Probabilities

Catalyst	α, specific		Avg.
Fe/HY	0.64(1.2)[a]	0.68(2.5) 0.66(3.0) 0.7(3.6)	0.67
Fe/NaY	0.61(1.1)	0.62(1.3) 0.18(1.9) 0.58(2.9)	0.59
Co/HY	0.59(0.7)	0.61(1.1) 0.63(2.0) 0.61(3.1)	0.61
Co/NaY	0.54(0.7)	0.53(1.2) 0.61(2.1) 0.55(3.0)	0.56
FeCo/HY	0.65(1.1)	0.59(1.8) 0.57(2.9) 0.56(3.8)	0.59
FeY	0.51(1.8)	0.5(3.0) 0.49(4.3) 0.5(5.8)	0.50
FeCoY	0.47(1.4)	0.53(2.7) 0.51(3.2) 0.53(3.9)	0.51
Fe/SiO_2[b]	0.47(0.9)	0.49(2.7) 0.5(4.6)	0.49
Co/SiO_2[b]	0.57(1.0)	0.61(2.0) 0.57(3.0)	0.58
$FeCo/SiO_2$[b]	0.52(1.9)	0.54(3.9)	0.53

[a] Number in parentheses is conversion level of CO (%); α determined for C_2–C_9 products.

[b] Data of Arcuri *et al.* (9).

DISCUSSION AND CONCLUSIONS

Several points are of interest concerning the Y-supported catalysts both in terms of intrinsic properties and in comparison to similar SiO_2 materials. These are summarized below.

(1) The Mössbauer spectra of the ion-exchanged catalysts suggest that all of the iron ions locate in the hexagonal prism (site I), or possibly the sodalite cages (sites I', II') (*5*). These are not reduced beyond Fe^{2+} with H_2,425°,24, and are in accord with *Hurst et al.* (*20*) on the relative reducibility of metal ions on Y zeolite, and the reversibility of Fe^{2+}–Fe^{3+} on redox cycling. It is fairly clear for impregnated samples that large particles are external to the pore structure and are, thus, more easily reduced. This is confirmed by the Mössbauer data. However, carburization seems to be supressed. There is only ca. 20% carbide phase for Fe/HY, compared to almost 100% for comparable Fe/SiO_2 catalysts.

(2) In contrast to Fe/SiO_2 (*9*), no FeCo alloy is found in FeCo/HY after reduction (Fig. 2B). This agrees with the results of Suib *et al.* (*3*) for FeCo on zeolite support. It has been proposed that the interaction between metal and zeolite approaches that of a metal–semiconductor contact with zeolite as an electron acceptor (*21, 22*). On this basis a strong metal–support interaction might be expected that inhibits alloy formation.

(3) Table 7 shows that the zeolite-supported catalysts yield more high-molecular-weight products, and that the ratio of ethylene to ethane turnover drops significantly from 2.0 for SiO_2 to 0.4 for HY. Dejaifve *et al.* (*23*) proposed a carbenium ion mechanism with ethylene protonation via Brønsted acid sites to form carbenium-like surface species. This intermediate can then react further to form high-molecular-weight products. The present results are consistent with this. HY is abundant in Brønsted sites (*23*) and even for NaY there are still sites of this type though isomer formation is lower, as expected. Since the metallic particles are large and external to the zeolite pore structure, it would be of interest to investigate mechanical mixtures of metal and zeolite to see if similar product distributions are obtained.

(4) For higher molecular weight products, C_5^+, only about 5% isomers were found with SiO_2-supported catalysts (*9*), while here over 80% of the C_5^+ material consisted of isomerized products. Table 7 gives the total production of C_5^+; details of the individual compositions through C_8 are given in (*15*). The high ratio of isomerized products for the acidic Y is obviously enhanced by the abundance of Brønsted sites in HY (*23*).

(5) With the exception of an irregular drop at C_2 (noted for other catalysts) the chain growth propagation model is obeyed for the Y-supported catalysts. The α values for Fe/HY compared to Fe/SiO_2 are much higher, while those for Co on the two supports are about the same, with FeCo intermediate. A consequence is that Fe/HY becomes the most efficient long-chain producer in the Y series, whereas Co was markedly better in this respect for the SiO_2 series.

(6) Specific comparison of the Y-supported Fe catalysts with their silica-supported counterparts can be summarized as follows.

(i) Impregnated Y-supported catalysts have higher activity, α values, and isomerization activity compared to SiO_2 materials. Isomer formation is supressed on NaY, but still present.

(ii) Ion-exchanged Y materials cannot be reduced to Fe°, whereas ca. 90% reduction is obtained for silica-supported catalysts under the same conditions.

(iii) Full carburization is observed under reaction conditions for Fe/SiO_2, while only partial formation of carbide phases is observed for Fe/HY. The stronger metal–support interaction in the zeolite-supported series inhibits carbide formation.

(iv) Similarly, the zeolite support seems

to inhibit FeCo alloy formation. The resulting low-molecular-weight olefin/paraffin ratios are similar for FeCo/HY and Fe/HY, and differ considerably from Fe/SiO_2 (Table 8). The characteristics of the "bimetallic" FeCo on Y zeolite are, thus, dominated by Fe.

(v) The much higher α values for Fe/HY vs Fe/SiO_2 are not easily explained. One major difference between the two is the extent of carburization under reaction conditions, providing some evidence of a role of carbide in suppressing chain growth. For Co/SiO_2 there is no carbide formation and α is greater than for Fe/SiO_2; when carbide formation is inhibited, as for Fe/HY, α is greatly enhanced. This behavior may, however, also be attributed in part to participation of the zeolite in the chain growth mechanism via the high surface acidity and corresponding ionic polymerization activity (*23*).

ACKNOWLEDGMENTS

This research was supported in part by the Exxon Education Foundation and by the Department of Energy, Office of Basic Energy Sciences, Contract DE-AC02-78ER0-4973. Mössbauer and X-ray studies were carried out in the Northwestern Materials Research Center facilities, supported by NSF MRL Contract DMR82-16972. We are indebted to Dr. K. Huang for the CO chemisorption measurements.

REFERENCES

1. Ballivet-Tkatchenko, D., Coudurier, G., Mozazanega, H., and Tkatchenko, I., *J. Mol. Catal.* **6,** 293 (1979).
2. Melson, G. A., Crawford, J. E., and Crites, J. W., *in* "Intrazeolite Chemistry" (G. D. Stucky and F. G. Dwyer, Eds.), ACS Symp. Ser., Vol. 218, p. 397. Amer. Chem. Soc., Washington, D.C., 1983.
3. Suib, S. L., McMahon, K. C., Tau, L. M., and Bennett, C. O., *J. Catal.* **89,** 20 (1984).
4. Chang, C. D., Lang, W. H., and Silvestri, A. J., *J. Catal.* **56,** 268 (1979).
5. Leith, I. R., CSIR Report CEG 218, Linde Molecular Sieves (1977).
6. Gates, B. C., Katzer, J. R., and Schuit, G. C. A., "Chemistry of Catalytic Processes," p. 55. McGraw–Hill, New York, 1979.
7. Amelse, J. A., Schwartz, L. H., and Butt, J. B., *J. Catal.* **72,** 95 (1981).
8. Shorman, J. D., *AIChE Symp. Ser.* **74,** 98 (1978).
9. Arcuri, K. B., Piotrowski, R. B., Schwartz, L. H., and Butt, J. B., *J. Catal.* **85,** 349 (1984).
10. Amelse, J. A., Butt, J. B., and Schwartz, L. H., *J. Phys. Chem.* **82,** 558 (1978).
11. Amelse, J. A., Grynkevich, G., Butt, J. B., and Schwartz, L. H., *J. Phys. Chem.* **85,** 2484 (1981).
12. Delgass, W. N., Garten, R. L., and Boudart, M., *J. Phys. Chem.* **73,** 2970 (1969).
13. Garten, R. L., Delgass, W. N., and Boudart, M., *J. Catal.* **18,** 90 (1970).
14. Segawa, K. I., Chen, Y., Kubsh, J. E., Delgass, W. N., Dumesic, J. A., and Hall, W. K., *J. Catal.* **76,** 112 (1982).
15. Lin, T-S., PhD dissertation. Northwestern University, Evanston, Illinois, 1984.
16. Petunchi, J. O., and Hall, W. K., *J. Catal.* **78,** 327 (1982).
17. Nandi, R. K., Molinaro, F., Cohen, J. B., Butt, J. B., and Burwell, R. L., Jr., *J. Catal.* **78,** 289 (1982).
18. Shashital, S. K., Cohen, J. B., Burwell, R. L., Jr., and Butt, J. B., *J. Catal.* **50,** 479 (1977).
19. Biloen, P., and Sachtler, W. M. H., "Advances in Catalysis," Vol. 30, p. 165., Academic Press, New York, 1981.
20. Hurst, N. W., Gentry, S. J., and Jones, A., *Catal. Rev.* **24,** 2333 (1982).
21. Rabo, J. A., *Catal. Rev.* **23,** 293 (1981).
22. Anderson, J. R., "Structure of Metallic Catalysts," p. 277. Academic Press, New York, 1975.
23. Dejaifve, P., Vedrine, J. C., Babis, V., and Derouaine, E. G., *J. Catal.* **63,** 31 (1980).